Bin Feng,[1] Ping Jiao,[1,2] Ynes Helou,[3] Yujie Li,[1] Qin He,[1] Matthew S. Walters,[4] Arthur Salomon,[5,6] and Haiyan Xu[1,7]

# Mitogen-Activated Protein Kinase Phosphatase 3 (MKP-3)–Deficient Mice Are Resistant to Diet-Induced Obesity

Diabetes 2014;63:2924–2934 | DOI: 10.2337/db14-0066

METABOLISM

**Mitogen-activated protein kinase phosphatase 3 (MKP-3) is a negative regulator of extracellular signal–related kinase signaling. Our laboratory recently demonstrated that MKP-3 plays an important role in obesity-related hyperglycemia by promoting hepatic glucose output. This study shows that MKP-3 deficiency attenuates body weight gain induced by a high-fat diet (HFD) and protects mice from developing obesity-related hepatosteatosis. Triglyceride (TG) contents are dramatically decreased in the liver of MKP-3$^{-/-}$ mice fed an HFD compared with wild-type (WT) controls. The absence of MKP-3 also reduces adiposity, possibly by repressing adipocyte differentiation. In addition, MKP-3$^{-/-}$ mice display increased energy expenditure, enhanced peripheral glucose disposal, and improved systemic insulin sensitivity. We performed global phosphoproteomic studies to search for downstream mediators of MKP-3 action in liver lipid metabolism. Our results revealed that MKP-3 deficiency increases the phosphorylation of histone deacetylase (HDAC) 1 on serine 393 by 3.3-fold and HDAC2 on serine 394 by 2.33-fold. Activities of HDAC1 and 2 are increased in the livers of MKP-3$^{-/-}$ mice fed an HFD. Reduction of HDAC1/2 activities is sufficient to restore TG content of MKP-3$^{-/-}$ primary hepatocytes to a level similar to that in WT cells.**

Obesity has become a major public health issue and is mainly caused by a sedentary lifestyle and energy-dense diet. Massive expansion of white adipose tissue (WAT) is the hallmark of obesity. Excessive energy is normally stored in WAT as triglycerides (TGs). Lipids are deposited into nonadipose tissues such as liver and muscle when the limit of WAT storage capacity is reached. Lipotoxicity is a major causal factor for the development of insulin resistance; it promotes the production of inflammatory mediators in WAT and the liver (1,2). The effect of insulin on glycemic control is implemented through coordinated actions in multiple tissues. In the liver, insulin represses glucose output (3); in muscle and fat, insulin stimulates glucose uptake (4,5). In the state of insulin resistance, glucose output from the liver increases, and glucose disposal in muscle and fat decreases. As a result, circulating insulin levels must increase to maintain a blood glucose concentration within the normal range. Whether an individual with insulin resistance ultimately develops diabetes depends on the capacity of pancreatic β-cells to sustain increased insulin secretion (6).

The liver is an important organ for maintaining energy homeostasis. It keeps blood glucose concentrations within a normal range by promoting glycogenesis (sequestering glucose by glycogen synthesis) after a meal and activating glycogenolysis (breakdown of glycogen) and gluconeogenesis from noncarbohydrate precursors during starvation (7). The liver is also central for lipid metabolism. It is highly active in oxidizing TGs to produce energy and

[1]Hallett Center for Diabetes and Endocrinology, Rhode Island Hospital, Brown University, Warren Alpert Medical School, Providence, RI
[2]School of Pharmaceutical Sciences, Jilin University, Changchun, Jilin Province, China
[3]Department of Molecular Pharmacology and Physiology, Brown University, Providence, RI
[4]Department of Genetic Medicine, Weill Cornell Medical College, New York, NY
[5]Department of Molecular Biology, Cell Biology and Biochemistry, Brown University, Providence, RI
[6]Department of Chemistry, Brown University, Providence, RI
[7]Pathobiology Program, Brown University, Providence, RI

Corresponding author: Haiyan Xu, hxu@lifespan.org.

Received 15 January 2014 and accepted 3 April 2014.

This article contains Supplementary Data online at http://diabetes.diabetesjournals.org/lookup/suppl/doi:10.2337/db14-0066/-/DC1.

exports through circulation large quantities of acetoacetate to be metabolized by other tissues. It is also the main site for converting excessive carbohydrates and proteins into free fatty acids and TGs, which are subsequently transported to adipose tissue for storage. In the setting of overnutrition, liver and adipose tissue have been considered the primary organs for systemic metabolic disorders, whereas skeletal muscle and pancreatic islets are thought of as responder systems (8).

Mitogen-activated protein (MAP) kinase phosphatases (MKPs) are negative regulators of the MAP kinase pathway in the regulation of mitogenesis. Our study is the first to reveal the involvement of MKP in insulin-regulated metabolic pathways. We previously reported that MKP-3 is highly upregulated in the liver of obese and diabetic mice and promotes glucose output in both cultured liver cells of rats and in the livers of mice (9,10). In this study, we characterized the metabolic phenotype of MKP-$3^{-/-}$ mice in response to overnutrition. Global MKP-3 deficiency not only decreases blood glucose concentrations and significantly improves systemic insulin sensitivity but also reduces TG contents in both the liver and WAT, indicating that MKP-3 is involved in both glucose and lipid metabolism. Through phosphoproteomic study, we identified that MKP-3 regulates lipogenesis in the liver through modulation of histone deacetylase (HDAC) 1/2 phosphorylation.

## RESEARCH DESIGN AND METHODS

### Reagents and Cells

Hepa1–6 mouse hepatoma cells were provided by Dr. Gökhan Hotamisligil (Harvard School of Public Health). 3T3-L1 cells were purchased from the American Type Culture Collection. 3T3-L1 coxsackie and adenovirus receptor (3T3-L1 CAR) cells were provided by Dr. David Orlicky (University of Colorado Health Sciences Center) (11). Preadipocytes were differentiated using a previously described method (12). Mouse insulin ELISA kits were purchased from ALPCO (Salem, NH). MKP-3 antibody (Ab), HDAC1 and 2 Abs, and hemagglutinin Ab were purchased from Santa Cruz Biotechnology (Santa Cruz, CA). Flag Ab was purchased from Sigma-Aldrich (St. Louis, MO). Tubulin Ab was purchased from Abcam. Insulin, dexamethasone, isobutyl methyl xanthine, ATP, horseradish peroxidase, glycerol phosphate oxidase, glycerol kinase, and lipase were purchased from Sigma-Aldrich. Acyl CoA oxidase was purchased from Wako Diagnostics (Richmond, VA). Amplex red was purchased from Invitrogen (Carlsbad, CA). Humulin R was purchased from Eli Lilly (Indianapolis, IN). Glucose test strips and AlphaTRAK meters were purchased from Abbott Animal Health (Abbott Park, IL). Fluorogenic HDAC Assay Kits were purchased from BPS Bioscience (San Diego, CA). HDAC1 and 2 constructs were provided by Dr. Matthew S. Walters (Weill Cornell Medical College). Luciferase kits were purchased from Promega (Madison, WI). FK228 and SAHA were purchased from Selleckchem.com (Houston, TX).

### Isolation of Primary Cells

Adipocytes and stromal vascular cells were isolated from gonadal fat pads of mice using a method described previously (12). For in vitro adipogenesis, stromal vascular cells were seeded on 24-well plates at a density of $4 \times 10^5$/well and induced by DMEM containing 10% cosmic calf serum, 0.5 mmol/L isobutyl methyl xanthine, 1 μmol/L dexamethasone, and 1 μg/mL insulin. Primary hepatocytes were isolated by infusing mouse liver with collagenase buffer, and cells were filtered through a 150-μm tissue sieve. Cells were seeded in collagen-coated 6-well plates at a density of $1 \times 10^6$/well.

### Hyperinsulinemic-Euglycemic Clamp Study

Catheters were implanted into the left jugular vein of mice 5–10 days before the clamp study. After an overnight fast, a hyperinsulinemic-euglycemic clamp study was performed using a method described previously (10).

### RNA Extraction and Real-Time PCR Analysis

RNA samples were extracted from tissues or isolated cells using the TRIzol reagent (Invitrogen) according to the manufacturer's instructions. Real-time PCR analysis was performed using a method described previously (10).

### Immunoprecipitation and Immunoblot Blot Analysis

Tissues and cells were homogenized and lysed with ice-cold lysis buffer supplemented with protease inhibitors. MKP-3 was immunoprecipitated using a method described previously (10). Protein lysates were separated on 4–12% Bis-Tris-PAGE gel and transferred onto polyvinylidene difluoride membranes. Following blocking, membranes were incubated with the corresponding primary antibodies. After thorough washes, membranes were exposed to corresponding horseradish peroxidase–linked secondary antibodies, and signals were detected with a chemiluminescence Western blotting detection solution (PerkinElmer, Waltham, MA) using the α-Innotech fluorochem image system.

### Mice Maintenance and Analysis

MKP-3–deficient male mice were purchased from The Jackson Laboratory (Bar Harbor, ME); they were maintained on a mixed B6/129 background. We backcrossed them with C57BL/6 female mice purchased from The Jackson Laboratory for nine generations. Mice were kept on a 12-h light/dark cycle and given ad libitum access to food and water. Mice were fed on either a normal chow diet or a high-fat diet (HFD; 60% kcal from fat; D12492, Research Diets) at 4 weeks of age. The HFD was maintained for up to 28 weeks. Body weights were measured biweekly. At the end of study, mice were killed by asphyxiation with carbon dioxide ($CO_2$) after an overnight fast or under fed conditions. Plasma and tissues were collected for further analysis. All animal procedures used in our studies were approved by the Institutional Animal Care and Use Committee of Rhode Island Hospital.

### Histological Analysis

Livers were fixed in 10% neutrally buffered formalin for 1 day then transferred to 70% ethanol and embedded in

paraffin for sectioning. Hematoxylin-eosin and Oil red O staining were performed at the Rhode Island Hospital's core laboratory.

### Measurement of TG Contents

The TG contents in tissue were determined using homogenates of mesenteric WAT and liver samples. Frozen tissues were weighed, pulverized in liquid nitrogen, homogenized in ethanol, vortexed, and centrifuged; the supernatant was collected for measurement. To extract plasma TGs, plasma was vortexed in ethanol and centrifuged, and supernatant was gathered for measurement. To measure TG contents, TG standards or samples were mixed with reaction buffer and incubated for 30 min at 37°C.

### Indirect Calorimetry

Oxygen consumption ($VO_2$), $CO_2$ production ($VCO_2$), and food intake were measured individually for 24 h using the comprehensive laboratory animal monitoring system (Columbus Instruments, Columbus, OH) after 1 day of acclimation. During the experiment, mice had free access to food and water. Energy expenditure was calculated using the following formula: $VO_2 \times (3.815 + 1.232 \times \text{Respiratory Quotient})$, and normalized to $(\text{body mass})^{0.75}$.

### Insulin Tolerance Test

For the insulin tolerance test (ITT), mice were fasted for 6 h, and male mice fed an HFD were injected with insulin at a dose of 1 U/kg. Blood glucose concentrations were measured at 0, 15, 30, 45, 60, and 90 min after injection.

### Phosphoproteomic Study

Hepa1–6 cells were cultured in stable isotope labeling in cell culture (SILAC) medium for eight doublings and then seeded in SILAC medium on 6-well plates. Half of the cells were labeled with light arginine and lysine and infected with adenovirus expressing short hairpin interfering RNA against green fluorescent protein (shGFP). The other half were labeled with heavy arginine and lysine and infected with adenovirus expressing short hairpin interfering RNA against MKP-3. For each sample, 2.5 mg of protein lysates labeled with light arginine and lysine were mixed with 2.5 mg of protein lysates labeled with heavy arginine and lysine. Samples were reduced with 45 mmol/L dithiothreitol at 60°C for 20 min, alkylated with 100 mmol/L iodoacetimide for 15 min in the dark, and digested overnight with TPCK-treated trypsin. Peptides then were desalted using Sep-Pak C18 columns and enriched for phosphopeptides using a Titansphere Phos-TiO kit before loading to an Orbitrap Velos electron transfer dissociation mass spectrometer. Results from five biological replicates were used for data analysis. *Q* values for multiple hypothesis tests also were calculated based on the determined *P* values using the R package QVALUE, as previously described (13).

### HDAC Activity Assay

HDAC1 or 2 was immunoprecipitated, and activity was assayed using the fluorogenic HDAC assay kit from BPS Bioscience, according to the manufacturer's instructions. Immunoprecipitation beads were washed four times with lysis buffer and twice with HDAC assay buffer then incubated with 50 μL HDAC substrate at 37°C for 30 min. After centrifugation, 30 μL supernatant was mixed with 30 μL developer for 15 min of incubation at room temperature. Fluorescence was read at excitation 360 nmol/L and detection 450 nmol/L.

### Statistical Analysis

Results are presented as mean ± standard errors. Statistical significance was determined at $P < 0.05$. Student *t* test was used to compare differences between two groups. Two-way ANOVA and Bonferroni posttests were used to analyze multiple experimental groups.

## RESULTS

### MKP-3 Deficiency Protects Mice From Developing Diet-Induced Obesity

MKP-$3^{-/-}$ mice are significantly lighter than wild-type (WT) littermates (controls) at 4 weeks of age (Fig. 1*A*). When fed a chow diet, MKP-$3^{-/-}$ mice became indistinguishable from WT mice between 6 and 20 weeks of age (Fig. 1*A*). After 23 weeks of age, male MKP-$3^{-/-}$ mice became significantly leaner than WT mice (Supplementary Fig. 1*A*). When challenged with an HFD, body weight gain is attenuated by MKP-3 deficiency in both sexes (Fig. 1*B*), and mice are protected from developing diet-induced obesity (DIO). Concentrations of fasting blood glucose and fasting plasma insulin are significantly lower in MKP-$3^{-/-}$ mice fed an HFD compared with WT mice (Fig. 1*C* and *D*). There is no difference in fasting blood glucose and fasting plasma insulin concentrations between WT and MKP-$3^{-/-}$ mice fed a chow diet (Supplementary Fig. 1*B*). The ITTs indicate improved systemic insulin sensitivity in MKP-$3^{-/-}$ mice fed an HFD (Fig. 1*E*).

The weights of liver and total adipose tissue are significantly reduced in MKP-$3^{-/-}$ mice fed an HFD compared with WT controls (Fig. 2*A*). Weights of adipose tissue are significantly decreased in all fat depots of female MKP-$3^{-/-}$ mice fed an HFD and in all fat depots (except gonadal) of male MKP-$3^{-/-}$ mice fed an HFD (Supplementary Fig. 2*A*). MKP-3 deficiency did not change circulating lipid profiles (Fig. 2*B*). Liver weights also are significantly reduced in MKP-$3^{-/-}$ mice fed a chow diet, but adipose tissue weights are only significantly decreased in male MKP-$3^{-/-}$ mice fed a chow diet; there is no significant change in female MKP-$3^{-/-}$ mice receiving chow (Supplementary Fig. 2*B* and *C*). TG contents in the livers of MKP-$3^{-/-}$ mice fed an HFD are drastically reduced to levels comparable to those in the livers of lean WT mice (Fig. 2*C*). TG contents in the livers of MKP-$3^{-/-}$ mice fed chow also are significantly reduced (Fig. 2*C*). Histology study reveals that MKP-3 deficiency protects mice from developing HFD-induced hepatosteatosis (Fig. 2*D*). Gene expression analysis demonstrates significant reduction of lipogenic gene expression, including fatty acid synthase (*FAS*), stearoyl CoA desaturase 1 (*SCD1*), acetyl CoA carboxylase 2 (*ACC2*), and peroxisome proliferator-activated receptor γ (*PPARγ*) in MKP-$3^{-/-}$ mice fed an HFD

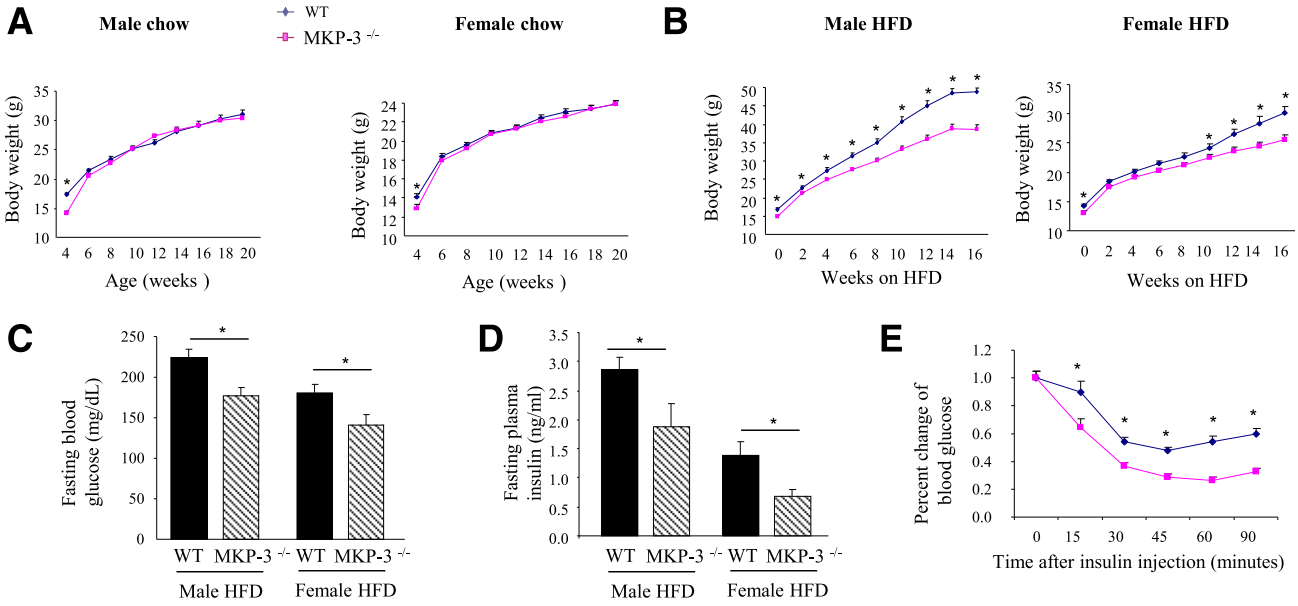


**Figure 1**—MKP-3$^{-/-}$ mice are resistant to DIO. *A*: Growth curves of WT and MKP-3$^{-/-}$ mice receiving a chow diet ($n$ = 10–15 per group). *B*: Growth curves of WT and MKP-3$^{-/-}$ mice receiving an HFD ($n$ = 11 for male WT, $n$ = 10 for male MKP-3$^{-/-}$, $n$ = 13 for female WT, and $n$ = 7 for female MKP-3$^{-/-}$ mice). *C*: Fasting blood glucose levels of WT and MKP-3$^{-/-}$ mice fed an HFD ($n$ = 7 per group). *D*: Fasting plasma insulin levels of WT and MKP-3$^{-/-}$ mice fed an HFD ($n$ = 6 or 7 per group). *E*: ITT of male mice fed an HFD for 16 weeks ($n$ = 7). *$P$ < 0.05, WT vs. MKP-3$^{-/-}$.

compared with WT mice fed an HFD (Fig. 2*E*). To determine whether MKP-3 is required for transcription of lipogenic genes, FAS promoter-driven luciferase reporter construct was transfected into cultured mouse hepatoma Hepa1–6 cells expressing interfering RNA for green fluorescent protein (shGFP) or MKP-3 (shMKP-3). Transcription of FAS promoter is significantly repressed when expression of MKP-3 is reduced (Fig. 2*F*).

### Absence of MKP-3 Increases Energy Expenditure and Improves Glucose Homeostasis

To understand the effect of MKP-3 deficiency on whole-body energy homeostasis, metabolic cages were used. Oxygen consumption, $CO_2$ release, and energy expenditure are significantly increased during a 24 h period in both male and female MKP-3$^{-/-}$ mice fed an HFD (Fig. 3*A*). Further analysis indicates that these parameters significantly increase during both dark and light cycles (data not shown). Food intake is not changed in male MKP-3$^{-/-}$ mice fed an HFD but is significantly increased in female MKP-3$^{-/-}$ mice fed an HFD (Fig. 3*A*). The respiratory exchange ratio remains unchanged, indicating that the balance between lipid and carbohydrate oxidation does not shift. Oxygen consumption, $CO_2$ release, and energy expenditure also are significantly increased during the dark period in MKP-3$^{-/-}$ male mice fed a chow diet but not changed in MKP-3$^{-/-}$ female mice fed a chow diet (data not shown). Food intake does not change in either sex when fed a chow diet (data not shown).

Hyperinsulinemic-euglycemic clamp study demonstrates significantly increased glucose infusion rate in MKP-3$^{-/-}$ female mice fed an HFD (Fig. 3*B*), supporting our previous conclusion, based on the results of ITTs, that systemic insulin sensitivity is improved in the absence of MKP-3. Hepatic glucose production can be more effectively suppressed by insulin in MKP-3$^{-/-}$ mice (Fig. 3*B*). Glucose disposal rate also is significantly improved in MKP-3$^{-/-}$ mice; this is most likely attributable to increased muscle glucose uptake and glycolysis (Fig. 3*B*). Glucose uptake in WAT increased 54.8% but did not reach statistical significance (Fig. 3*B*). Plasma insulin levels in MKP-3$^{-/-}$ female mice fed an HFD are significantly lower than those of WT mice during the clamp period (Fig. 3*C*).

### MKP-3 Plays a Role in Adipocyte Differentiation

MKP-3 mRNA level has been previously reported to increase in WAT of ob/ob and db/db mice (9). In this study, levels of MKP-3 mRNA and protein expression are shown to significantly increase in WAT of mice with DIO (Fig. 4*A* and *B*). Interestingly, the level of MKP-3 protein expression significantly increases at the early stage of adipogenesis (2 days after induction; Fig. 4*C*), suggesting that MKP-3 may play a role in adipocyte differentiation. Adipogenesis of 3T3-L1 coxsackie and adenovirus receptor adipocytes (a subline of 3T3-L1 that stably expresses the truncated adenovirus receptor) is impaired when MKP-3 expression was reduced in preadipocytes by adenovirus-mediated expression of interfering RNA against MKP-3 (shMKP-3), as shown by decreased TG accumulation (Fig. 4*D*). Analysis of gene expression reveals significant reduction of peroxisome proliferator-activated receptor γ, *FAS*, and *SCD1* (Fig. 4*E*). The stromal vascular cells isolated from gonadal adipose tissue of MKP-3$^{-/-}$ mice also display impaired adipogenesis, which

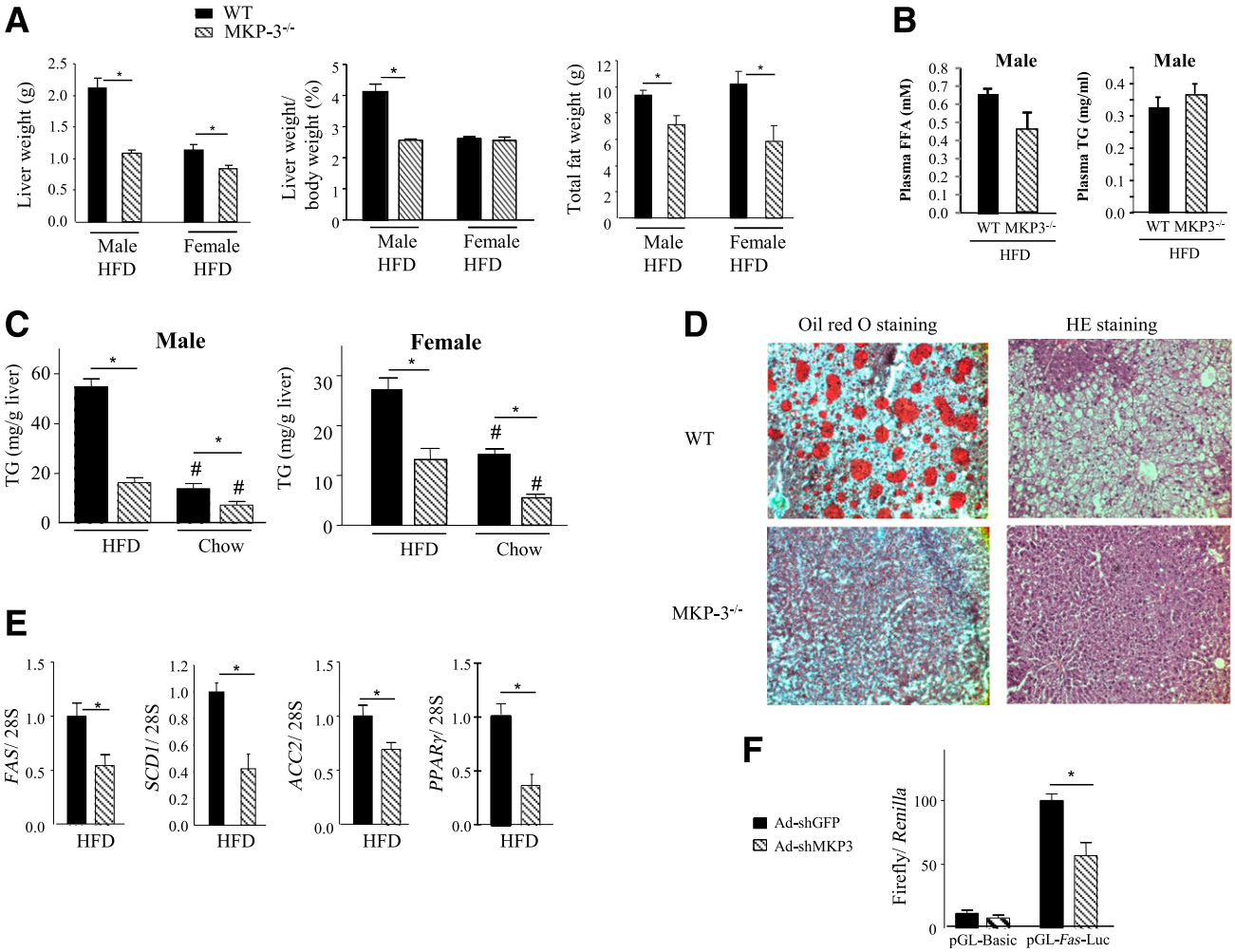


**Figure 2—** MKP-3 deficiency prevents HFD-induced hepatosteatosis. *A*: Weight of liver and total adipose tissue of WT and MKP-3$^{-/-}$ mice fed an HFD ($n$ = 6 or 7 per group). *B*: Circulating free fatty acid (FFA) and TG concentrations in WT and MKP-3$^{-/-}$ male mice fed an HFD ($n$ = 3–7 per group). *C*: Liver TG contents in WT and MKP-3$^{-/-}$ mice fed an HFD or chow ($n$ = 7 for male WT fed an HFD, $n$ = 6 for male MKP-3$^{-/-}$ fed an HFD, $n$ = 5 for male WT fed chow, $n$ = 9 for male MKP-3$^{-/-}$ fed chow, $n$ = 7 for female WT fed an HFD and MKP-3$^{-/-}$ HFD, $n$ = 10 for female WT fed chow, and $n$ = 8 for female MKP-3$^{-/-}$ fed chow). *D*: Liver histology of male WT and MKP-3$^{-/-}$ mice fed an HFD. HE, hematoxylin and eosin. *E*: Lipogenic gene expression in the livers of male WT and MKP-3$^{-/-}$ mice fed an HFD ($n$ = 7 or 8 per group). *F*: MKP-3 is essential for transcription of *FAS* promoter. Hepa1–6 cells were transfected with pCMV-*Renilla* control vector plus pGL3-Basic or pGL3-*FAS*-promoter using the Fugen HD transfection reagent. The next day, cells were infected with Ad-shGFP or Ad-shMKP-3. Luciferase assay was performed using Promega's duel luciferase assay kit. The ratio of luminescence from the *FAS* promoter (firefly) to luminescence from the control reporter (pCMV-*Renilla*) was calculated. The results shown here represent 3 independent experiments. $^{*}P < 0.05$, WT vs. MKP-3$^{-/-}$, or Ad-shGFP vs Ad-shMKP-3. $^{\#}P < 0.05$, diet-induced obese vs. lean mice. Luc, luciferase, *SCD1*, stearoyl CoA desaturase 1; *ACC2*, acetyl CoA carboxylase 2; *PPARγ*, peroxisome proliferator-activated receptor γ.

was reflected by significantly decreased expression of adipocyte genes such as CCAAT/enhancer binding protein α (*C/EBPα*), *FAS*, and *SCD1* (Fig. 4*F*). That baseline extracellular signal–related kinase (ERK) activity mildly increases in the heart of MKP-3$^{-/-}$ mice and promotes myocyte proliferation has been previously reported (14). ERK phosphorylation significantly increased in gonadal fat, but was unchanged in mesenteric fat, of MKP-3$^{-/-}$ male mice fed an HFD (Fig. 5*A* and data not shown). Because MKP-3 deficiency did not affect the weight of gonadal fat but did decrease mesenteric fat, the reduction of adiposity is unlikely due to ERK activation. Phosphorylation status of ERK2 but not ERK1 is significantly increased in the livers of MKP-3$^{-/-}$ mice fed an HFD (Fig. 5*B*).

### HDAC1 and 2 Are Downstream Targets of MKP-3 Signaling in Hepatic Lipid Metabolism

To identify potential downstream mediator(s) of MKP-3 action in lipid metabolism, global phosphoproteomics was studied using the quantitative SILAC method. Cultured mouse hepatoma Hepa1–6 cells expressing shMKP-3 via adenovirus-mediated gene transfer were labeled with heavy arginine/lysine, and control cells expressing shGFP were labeled with light arginine/lysine. Changes in serine/threonine phosphorylation caused by reduced MKP-3

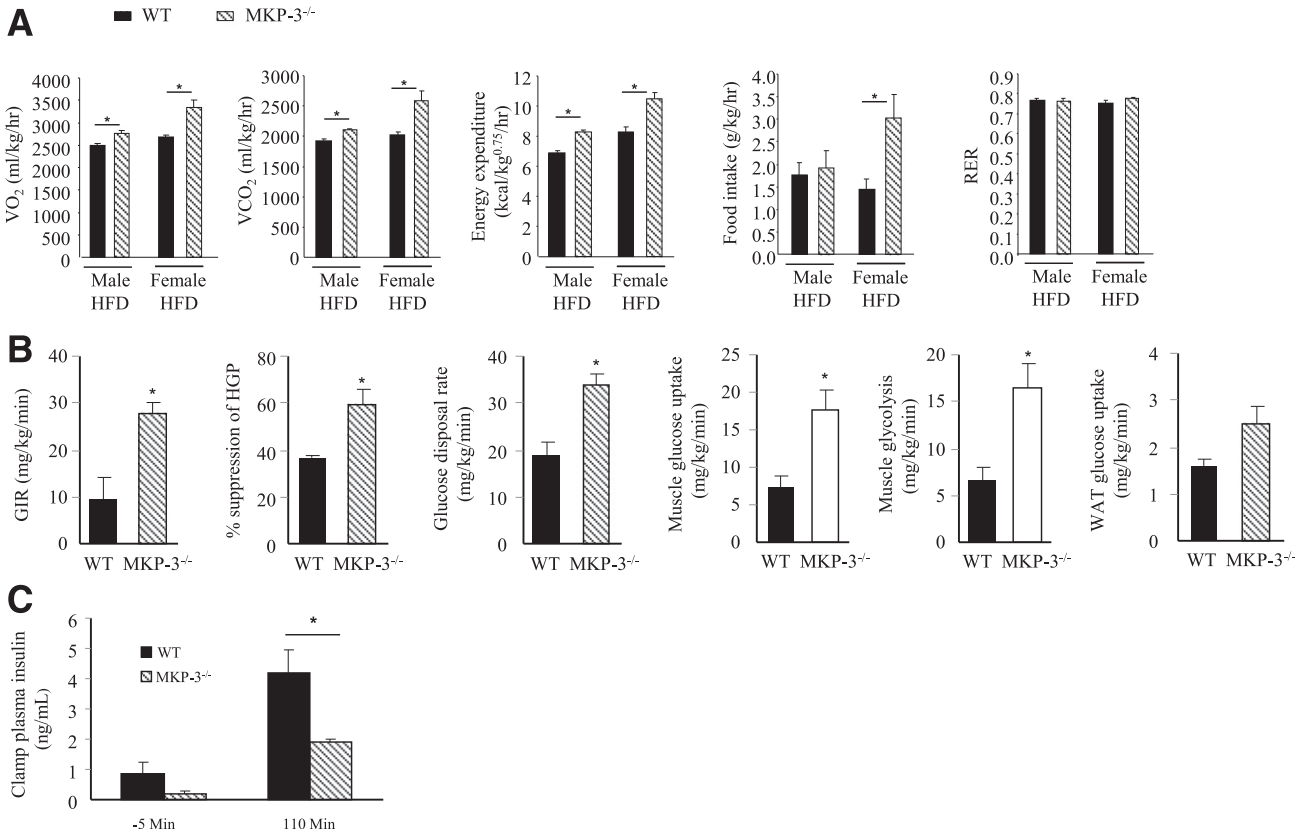


**Figure 3**—MKP-3 deficiency increases energy expenditure and improves glucose homeostasis. *A*: Oxygen consumption ($VO_2$), $CO_2$ release ($VCO_2$), energy expenditure, food intake, and respiratory exchange ratio (RER) of WT and MKP-$3^{-/-}$ male mice ($n$ = 4 per group) fed an HFD for 18 weeks. *B*: Hyperinsulinemic-euglycemic clamp study of WT and MKP-$3^{-/-}$ female mice fed an HFD for 28 weeks ($n$ = 3–6 per group). *C*: Plasma insulin concentrations during basal and clamp periods ($n$ = 3–6 per group). *$P < 0.05$, WT vs. MKP-$3^{-/-}$. GIR, glucose infusion rate; HGP, hepatic glucose production.

expression were expressed as ratios of shMKP-3 to shGFP. Under the condition of reduced expression of a phosphatase, we assume that phosphorylation levels of downstream mediators are increased if other phosphatases are not sufficient to compensate. Table 1 shows the average results of five biological replicates, which contain a total of 10 proteins with an increase in serine/threonine phosphorylation of 50% or more. Among these candidates, HDAC1 stood out as an interesting target, with significantly increased phosphorylation on serine 393 (S393) by 3.3-fold. Interestingly, our label-free global phosphoproteomic study using livers from WT and MKP-$3^{-/-}$ mice fed an HFD demonstrates significantly increased phosphorylation on serine 394 (S394) of HDAC2 by 2.33-fold due to the absence of MKP-3 (Supplementary Table 1).

HDAC1 and 2 proteins are 86% identical and 93% positive. S394 of HDAC2 is the equivalent of S393 of HDAC1. These two proteins are functionally redundant in many tissues (15–18). To understand the meaning of S393/S394 phosphorylation on HDAC1/2 activity, alanine and glutamic acid mutants were used in an activity assay. As shown in Fig. 6*A* and *B*, HDAC1 S393A/HDAC2 S394A mutants are significantly less active compared with WT proteins. Glutamic acid mutants partially mimic phosphorylation and are more active than alanine mutants but less active than WT proteins. The endogenous HDAC1/2 activities also are significantly increased in the livers of MKP-$3^{-/-}$ mice fed an HFD compared with WT controls, and this activity can be completely blocked by a pan HDAC inhibitor trichostatin A (Fig. 6*C*). Furthermore, endogenous HDAC1/2 activities are significantly decreased in the liver of WT mice fed an HFD compared with lean controls (Fig. 6*D*), consistent with our previous report that MKP-3 expression is markedly increased in the liver of mice with DIO (10). These results indicate that MKP-3 may repress HDAC1/2 activity by dephosphorylating HDAC1/2 on S393/S394. MKP-3 is predominantly localized in the cytoplasm but can shuttle between the nucleus and the cytosol (19). HDAC1/2 are nuclear enzymes but can be exported to the cytoplasm under pathological conditions (20,21). To test whether HDAC1 and 2 interact with MKP-3, HDAC1 and 2 were coexpressed with MKP-3 in Hepa1–6 cells. Both HDAC2 and MKP-3 could be immunoprecipitated with HDAC1 (Fig. 6*E*). Overexpression of the HDAC1 WT and S393E mutant, but not the S393A mutant, significantly suppresses expression of *SCD1* gene in Hepa1–6 cells (Fig. 6*F*).

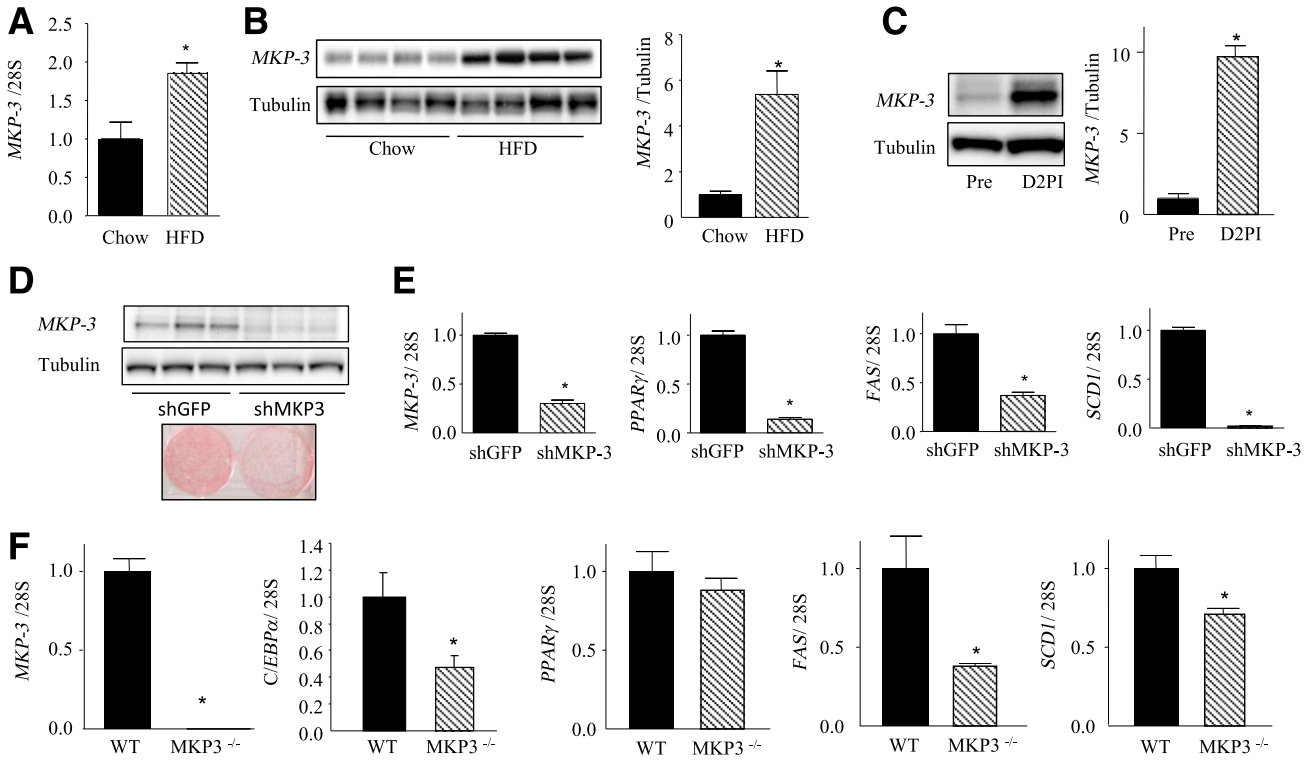


**Figure 4**—MKP-3 is involved in adipogenesis. *A*: MKP-3 mRNA expression in WAT in male mice fed an HFD or chow ($n$ = 4 per group). *B*: MKP-3 protein expression in WAT of mice fed an HFD or chow ($n$ = 4 per group). *C*: MKP-3 protein expression in 3T3-L1 cells 2 days after induction (D2PI) vs. preadipocytes (pre). *D* and *E*: MKP-3 knockdown in 3T3-L1 CAR preadipocytes and the effect on adipogenesis. *F*: Gene expression pattern during adipogenesis of stromal vascular cells isolated from WT or MKP-$3^{-/-}$ mice ($n$ = 3–4 per group). For cell-based experiments, results shown here are representative of 3 independent experiments. *$P < 0.05$, as indicated. *PPARγ*, peroxisome proliferator-activated receptor γ; *SCD1*, stearoyl CoA desaturase 1; c/*EBPα*, CCAAT/enhancer binding protein α.

To investigate whether increased HDAC1 and 2 activity in the liver of MKP-$3^{-/-}$ mice is responsible for decreased TG accumulation, we used both interfering RNA and a selective HDAC1/2 inhibitor to repress HDAC1/2 activity in liver cells. HDAC1 knockdown alone does not significantly increase the expression of lipogenic genes in Hepa1–6 cells. Reduction of HDAC2 expression alone significantly induces expression of both *SCD1* and *ACC2* genes. Reduction of both HDAC1 and HDAC2 significantly increases expression of *FAS*, *SCD1*, and *ACC2* genes (Fig. 7*A*). These results indicate that HDAC1 and 2 have a redundant function in repressing lipogenic gene expression. A potent and selective HDAC1/2 inhibitor, FK228, also was used to confirm the results obtained from interfering RNA against HDAC1 and 2. FK228 inhibited class I HDAC activity by more than 50% at a concentration of 5 nmol/L, whereas the pan HDAC inhibitor SAHA did not have any effect at the same concentration (Fig. 7*B*). FK228, not SAHA, significantly increases expression of *FAS*, *SCD1*, and *ACC2* genes at 5 nmol/L (Fig. 7*B*). Primary hepatocytes isolated from MKP-$3^{-/-}$ mice have a significantly reduced TG concentration (by 33%) compared with WT hepatocytes (Fig. 7*C*). Treatment with FK228 significantly increased TG concentration by 45% in WT hepatocytes but by 96% in MKP-$3^{-/-}$ hepatocytes, which completely abolishes the effect of MKP-3 deficiency on reducing TG accumulation (Fig. 7*C*). These results indicate that HDAC1 and 2 are likely the downstream mediators of MKP-3 action in lipid homeostasis.

## DISCUSSION

MKP-3 has a well-established role in the attenuation of MAP kinase signaling by selectively dephosphorylating ERK1/2 (22–24). Expression of hepatic MKP-3 drastically increases in response to overnutrition (10). One potential mechanism could be due to overnutrition-induced ERK activation (25). Our previous studies show that MKP-3 is an important regulator of hepatic gluconeogenesis by acutely overexpressing and knocking down MKP-3 in liver cells and in the liver of lean mice and mice with DIO via adenovirus-mediated gene transfer (9,10,26). In this study, the role of MKP-3 in whole-body energy homeostasis was investigated using global MKP-$3^{-/-}$ mice. As expected, MKP-3 deficiency significantly lowered fasting blood glucose concentrations and improved systemic insulin sensitivity in mice with DIO. In addition to the beneficial effect of phenotype on glycemic control, MKP-3 global deficiency protected mice from developing DIO, which could attribute to reduced adiposity, decreased hepatic lipid accumulation, and increased energy expenditure.

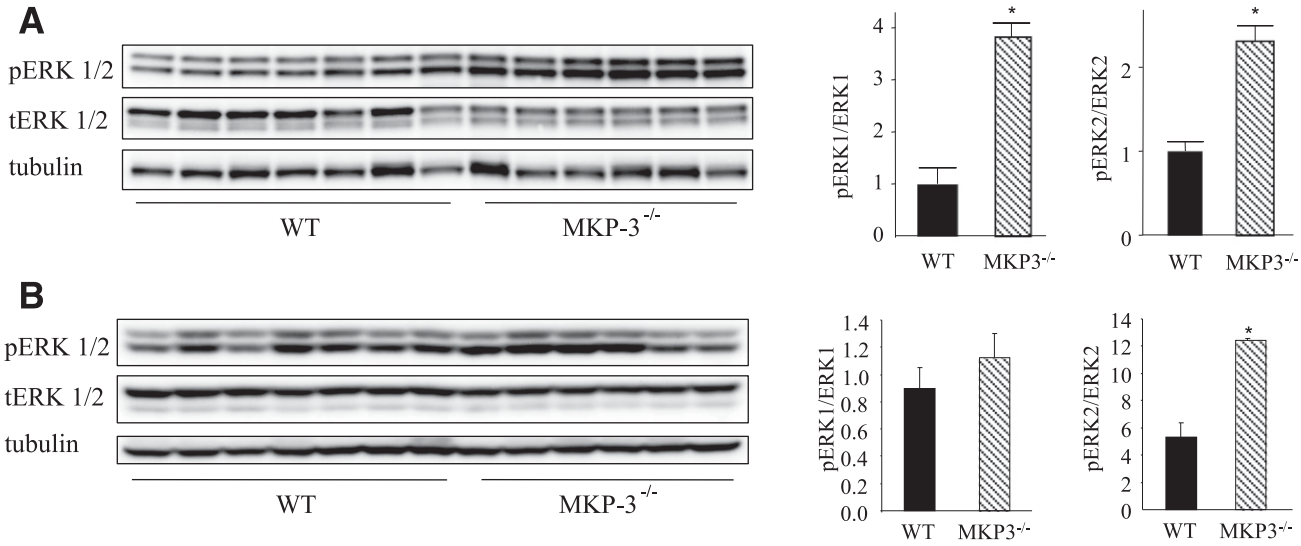


**Figure 5**—Effect of MKP-3 deficiency on basal ERK1/2 phosphorylation. *A*: Basal ERK1/2 phosphorylation in the gonadal adipose tissue of male WT and MKP-$3^{-/-}$ mice fed an HFD ($n$ = 6 or 7 per group). *B*: Basal ERK1/2 phosphorylation in the livers of male WT and MKP-$3^{-/-}$ mice fed an HFD ($n$ = 6 or 7 per group). *$P < 0.05$, WT vs. MKP-$3^{-/-}$.

Experiments with cultured adipocytes and isolated preadipocytes demonstrate that MKP-3 deficiency impairs in vitro adipocyte differentiation.

The major focus of this study is to investigate the underlying molecular mechanism of the protective effect of MKP-3 deficiency on HFD-induced hepatosteatosis. The liver TG contents in MKP-$3^{-/-}$ mice fed an HFD are similar to those in lean WT mice. These results indicate that MKP-3 plays a role in lipid homeostasis, which is a previously unrecognized and novel function. Considering the fact that the respiratory exchange ratio is not changed in MKP-$3^{-/-}$ mice, it is more likely that MKP-3 deficiency decreases lipogenesis. ERK2 activity is significantly increased in the liver of MKP-$3^{-/-}$ mice, but ERK2 is not likely to be responsible for the liver phenotype because, as we have previously shown, overexpression of the constitutively active mitogen-activated protein kinase kinase actually significantly increases liver weight (25). To

**Table 1—Fold increase of serine/threonine phosphorylation in mouse hepatoma cells with reduced MKP-3 expression vs. control cells**

| Symbol | Name | Phosphorylation sites | KD-to-control ratio | Q value for SILAC |
|---|---|---|---|---|
| Transcription | | | | |
| *HDAC1* | Histone deacetylase 1 | S393 | 3.3 | 0.02 |
| *THRAP3* | Thyroid hormone receptor–associated protein 3 | S935 | 1.5 | 0.04 |
| Translation repression | | | | |
| *EEF1D* | Eef1d protein | S162 | 2.7 | 0.02 |
| Ribosomal biogenesis | | | | |
| *NOP58* | Nucleolar protein 58 | S509 | 1.6 | 0.03 |
| Protein folding | | | | |
| *Ero1l* | Ero1l protein | S106 | 2.6 | 0.047 |
| Cytoskeleton | | | | |
| *PTK9* | Twinfilin-1 | S142 | 179 | 0.02 |
| Membrane trafficking | | | | |
| *SNX2* | Sorting nexin-2 | S97T101T104 | 9.4 | 0.03 |
| RNA processing | | | | |
| *PCBP1* | Poly(rC)-binding protein 1 | S173 | 2.5 | 0.047 |
| Function unknown | | | | |
| *RSRC2* | Rsrc2 arginine/serine-rich coiled-coil protein 2 isoform 1 | S32 | 2.0 | 0.02 |
| | AHNAK nucleoprotein isoform 1 | S136 | 1.5 | 0.03 |

KD, knockdown; SILAC, stable isotope labeling with amino acids in cell culture.

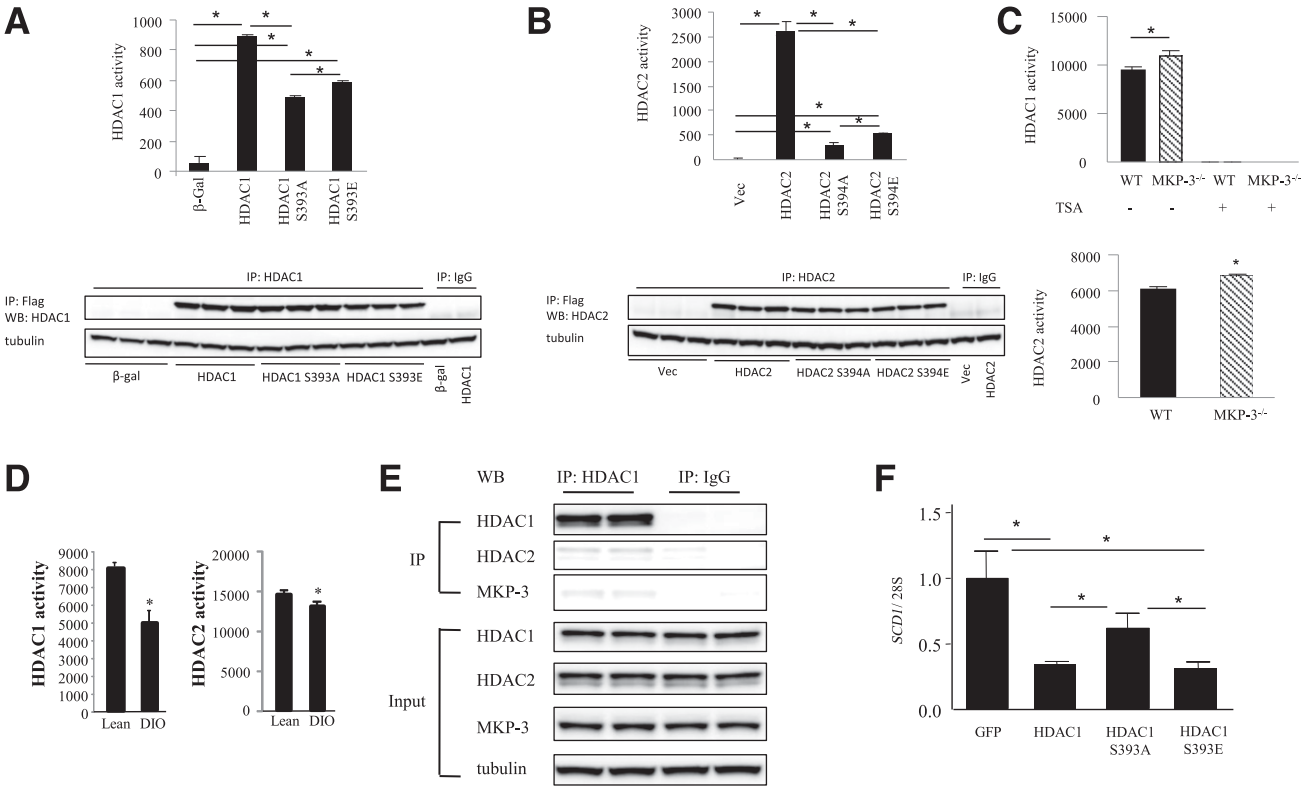


**Figure 6**—MKP-3 deficiency activates HDAC1/2. *A*: Effects of serine 393 mutants on HDAC1 activity in Hepa1–6 cells. *B*: Effects of serine 394 mutants on HDAC2 activity in Hepa1–6 cells. *C*: Hepatic HDAC1 and 2 activity in WT and MKP-3$^{-/-}$ mice fed an HFD ($n$ = 6 or 7 per group). *D*: Hepatic HDAC1 and 2 activity in WT mice fed a chow diet vs. an HFD ($n$ = 3–12 per group). *E*: HDAC1/HDAC2/MKP-3 interaction in Hepa1–6 cells. *F*: HDAC1 WT and HDAC1 S393E mutant, but not HDAC1 S393A mutant, reduces the expression of the endogenous *SCD1* gene in Hepa1–6 cells. For cell-based experiments, results shown represent 3 independent experiments. *$P$ < 0.05, as indicated. β-gal, β-glactosidase; TSA, tricostatin A; Vec, vector.

search for the downstream targets of MKP-3, we performed two phosphoproteomic studies to identify proteins with significantly increased phosphorylation in the absence of MKP-3: *1)* we compared stable isotope-labeled Hepa1–6 cells expressing shMKP-3 with cells expressing shGFP; *2)* we compared label-free liver lysates from MKP-3$^{-/-}$ mice fed an HFD with liver lysates from WT mice fed an HFD. The first experiment has less variation and represents acute reduction of MKP-3 expression. The second experiment is more physiologically relevant and reflects the status of chronic MKP-3 deficiency. Interestingly, one overlap is significantly increased phosphorylation of HDAC1 on S393 in experiment 1 and significantly increased phosphorylation of HDAC2 on S394 in experiment 2. We also demonstrate that activities of both HDAC1 and 2 are significantly decreased by an HFD. The expression of casein kinase 2α, which was reported to phosphorylate HDAC2 on S394 (27), is also significantly decreased by HFD (data not shown). This indicates that both MKP-3 and casein kinase 2α maybe responsible for decreased HDAC1/2 activity in response to overnutrition. Consistent with this hypothesis, HDAC1/2 activity is significantly increased by MKP-3 deficiency in the liver of mice with DIO, which is accompanied by decreased expression of lipogenic genes. These results indicate that HDAC1 and 2 may repress lipogenesis by inhibiting expression of lipogenic genes and that MKP-3 is required to keep HDAC1 and 2 in an unphosphorylated status on residues S393 and S394, respectively.

HDACs function as transcription repressors by deacetylating lysine residues on histone proteins, which results in chromatin condensation (28). HDACs are divided into three classes based on homology and function: class I (HDAC1–3, 8, 10), class II (4–7,9,11), and class III (sirtuins 1–7) (29). Among class I HDACs, HDAC1 and 2 are highly homologous and functionally redundant. Activities of HDAC1 and 2 can be modified by phosphorylation. It has been reported that phosphorylation on residues S421 and S423 promotes HDAC1 enzymatic activity (30). Previous publications also showed that casein kinase-2α1 promotes hypertrophic response in the heart by phosphorylating HDAC2 on S394. Our study reveals that phosphorylation on residue S393 of HDAC1 and S394 of HDAC2 are essential for their activity. The role of HDAC1 and 2 in liver lipid metabolism has not been investigated previously. Liver-specific deletion of HDAC3, also a class I HDAC, has been reported to cause hepatic lipid accumulation (31).

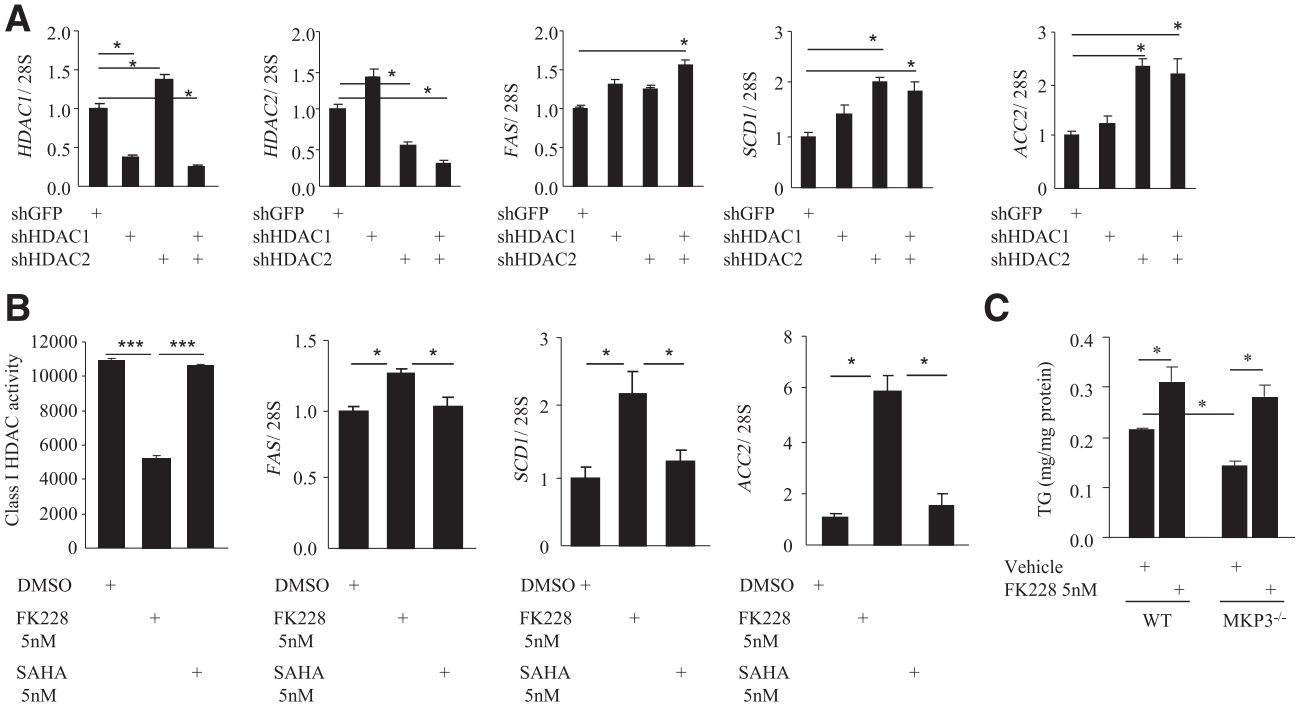


**Figure 7—**Reduction of HDAC1/2 activity increases lipogenesis in liver cells. *A*: Effects of HDAC1/2 knockdown on lipogenic gene expression in Hepa1–6 cells. *B*: Effects of selective HDAC1/2 inhibitor FK228 on lipogenic gene expression in Hepa1–6 cells. *C*: Effects of selective HDAC1/2 inhibitor FK228 on lipogenesis in primary hepatocytes isolated from WT or MKP-3$^{-/-}$ mice. For cell-based experiments, results shown here represent 3 independent experiments. *$P < 0.05$, as indicated; ***$P < 0.001$, as indicated.

Our results reveal for the first time that inactivation of HADC1/2 by either interfering RNA or the selective HDAC1/2 inhibitor FK228 is sufficient to promote lipogenic gene expression in liver cells. Most important, inactivation of HDAC1/2 in primary hepatocytes isolated from MKP-3$^{-/-}$ mice abolished the protective effect of MKP-3 deficiency on reducing TG content. These results support our hypothesis that MKP-3 is involved in lipid metabolism by regulating HDAC1/2 activity through modifying phosphorylation status on residues S393/S394. In an obese state, elevated MKP-3 expression in the liver likely contributes to hepatosteatosis by repressing the activity of HDAC1/2.

**Funding.** This work was supported by grants R01 DK080746 and R01 DK080746-02S1 from the National Institute of Diabetes and Digestive and Kidney Diseases. B.F. and P.J. are recipients of George A. Bray Research Scholars Awards from Brown University.

**Duality of Interest.** No potential conflicts of interest relevant to this article were reported.

**Author Contributions.** B.F., P.J., Y.H., Y.L., Q.H., A.S., and H.X. researched data. B.F., P.J., Y.H., M.S.W., and A.S. reviewed and edited the manuscript and contributed to the discussion. H.X. wrote the manuscript. H.X. is the guarantor of this work and, as such, had full access to all the data in the study and takes responsibility for the integrity of the data and the accuracy of the data analysis.

**Prior Presentation.** Parts of this study were presented in abstract form at the 2013 Keystone Symposia, Keystone, CO, 27 January–1 February 2013.

## References

1. Hotamisligil GS, Erbay E. Nutrient sensing and inflammation in metabolic diseases. Nat Rev Immunol 2008;8:923–934
2. Lomonaco R, Sunny NE, Bril F, Cusi K. Nonalcoholic fatty liver disease: current issues and novel treatment approaches. Drugs 2013;73:1–14
3. Saltiel AR, Kahn CR. Insulin signalling and the regulation of glucose and lipid metabolism. Nature 2001;414:799–806
4. Myers MG Jr, White MF. Insulin signal transduction and the IRS proteins. Annu Rev Pharmacol Toxicol 1996;36:615–658.
5. Holman GD, Kasuga M. From receptor to transporter: insulin signalling to glucose transport. Diabetologia 1997;40:991–1003
6. Rhodes CJ. Type 2 diabetes-a matter of beta-cell life and death? Science 2005;307:380–384
7. Pilkis SJ, Granner DK. Molecular physiology of the regulation of hepatic gluconeogenesis and glycolysis. Annu Rev Physiol 1992;54:885–909
8. Muoio DM, Newgard CB. Obesity-related derangements in metabolic regulation. Annu Rev Biochem 2006;75:367–401
9. Xu H, Yang Q, Shen M, et al. Dual specificity MAPK phosphatase 3 activates PEPCK gene transcription and increases gluconeogenesis in rat hepatoma cells. J Biol Chem 2005;280:36013–36018
10. Wu Z, Jiao P, Huang X, et al. MAPK phosphatase-3 promotes hepatic gluconeogenesis through dephosphorylation of forkhead box O1 in mice. J Clin Invest 2010;120:3901–3911
11. Orlicky DJ, DeGregori J, Schaack J. Construction of stable coxsackievirus and adenovirus receptor-expressing 3T3-L1 cells. J Lipid Res 2001;42:910–915
12. Jiao P, Chen Q, Shah S, et al. Obesity-related upregulation of monocyte chemotactic factors in adipocytes: involvement of nuclear factor-kappaB and c-Jun NH2-terminal kinase pathways. Diabetes 2009;58:104–115
13. Storey JD, Tibshirani R. Statistical significance for genomewide studies. Proc Natl Acad Sci U S A 2003;100:9440–9445

14. Maillet M, Purcell NH, Sargent MA, York AJ, Bueno OF, Molkentin JD. DUSP6 (MKP3) null mice show enhanced ERK1/2 phosphorylation at baseline and increased myocyte proliferation in the heart affecting disease susceptibility. J Biol Chem 2008;283:31246–31255
15. Montgomery RL, Davis CA, Potthoff MJ, et al. Histone deacetylases 1 and 2 redundantly regulate cardiac morphogenesis, growth, and contractility. Genes Dev 2007;21:1790–1802
16. Montgomery RL, Hsieh J, Barbosa AC, Richardson JA, Olson EN. Histone deacetylases 1 and 2 control the progression of neural precursors to neurons during brain development. Proc Natl Acad Sci U S A 2009;106:7876–7881
17. Yamaguchi T, Cubizolles F, Zhang Y, et al. Histone deacetylases 1 and 2 act in concert to promote the G1-to-S progression. Genes Dev 2010;24:455–469
18. LeBoeuf M, Terrell A, Trivedi S, et al. Hdac1 and Hdac2 act redundantly to control p63 and p53 functions in epidermal progenitor cells. Dev Cell 2010;19:807–818
19. Karlsson M, Mathers J, Dickinson RJ, Mandl M, Keyse SM. Both nuclear-cytoplasmic shuttling of the dual specificity phosphatase MKP-3 and its ability to anchor MAP kinase in the cytoplasm are mediated by a conserved nuclear export signal. J Biol Chem 2004;279:41882–41891
20. Kim JY, Shen S, Dietz K, et al. HDAC1 nuclear export induced by pathological conditions is essential for the onset of axonal damage. Nat Neurosci 2010;13:180–189
21. Bakin RE, Jung MO. HDAC2 cytoplasmic sequestration potentiates keratinocyte terminal differentiation. Open Cell Dev Biol J 2008;1:1–9
22. Camps M, Nichols A, Arkinstall S. Dual specificity phosphatases: a gene family for control of MAP kinase function. FASEB J 2000;14:6–16
23. Dickinson RJ, Keyse SM. Diverse physiological functions for dual-specificity MAP kinase phosphatases. J Cell Sci 2006;119:4607–4615
24. Zhao Y, Zhang ZY. The mechanism of dephosphorylation of extracellular signal-regulated kinase 2 by mitogen-activated protein kinase phosphatase 3. J Biol Chem 2001;276:32382–32391
25. Jiao P, Feng B, Li Y, He Q, Xu H. Hepatic ERK activity plays a role in energy metabolism. Mol Cell Endocrinol 2013;375:157–166
26. Jiao P, Feng B, Xu H. Mapping MKP-3/FOXO1 interaction and evaluating the effect on gluconeogenesis. PLoS One 2012;7:e41168
27. Segré CV, Chiocca S. Regulating the regulators: the post-translational code of class I HDAC1 and HDAC2. J Biomed Biotechnol 2011;2011:690848
28. Grunstein M. Histone acetylation in chromatin structure and transcription. Nature 1997;389:349–352
29. Ye J. Improving insulin sensitivity with HDAC inhibitor. Diabetes 2013;62:685–687
30. Pflum MK, Tong JK, Lane WS, Schreiber SL. Histone deacetylase 1 phosphorylation promotes enzymatic activity and complex formation. J Biol Chem 2001;276:47733–47741
31. Knutson SK, Chyla BJ, Amann JM, Bhaskara S, Huppert SS, Hiebert SW. Liver-specific deletion of histone deacetylase 3 disrupts metabolic transcriptional networks. EMBO J 2008;27:1017–1028